frontiers | Frontiers in Energy Research

METHODS
published: 11 May 2022
doi: 10.3389/fenrg.2022.901708

Black Start and Voltage Establishment Strategy for PMSG-Based Wind Turbine

Xiaotong Ji[1], Dan Liu[2], Pan Hu[2], Kan Cao[2], Kezheng Jiang[2], Guohang Huang[3]* and Sheng Huang[3]

[1]State Grid Hubei Electric Power CO., LTD., Wuhan, China, [2]Hubei Electric Power Research Institute, Wuhan, China, [3]College of Electrical and Information Engineering, Hunan University, Changsha, China

During the black start, backup ac power sources such as diesel generators can offer line-side voltage reference for wind turbine and keep line-side converter of wind turbine work properly so that the dc-link capacitor voltage within converter can be established without overcharge. This study proposes a black start control strategy and line-side voltage establishment method for PMSG-based wind turbines with no ac power source. Unlike the traditional control strategy of full power grid-connected converters, the dc-link voltage within back-to-back full power converters of wind turbines can be controlled by generator-side converters, and the line-side voltage can be established by line-side converters with the help of fixed loads. The mechanical power can be balanced by pitch angle control, and the power unbalance between mechanical power and electrical power will be reflected in the rotor speed of PMSG. By this method, a single wind turbine can establish the line-side voltage with no extra backup ac power source, offering voltage reference for the other wind turbines during the black start of a wind power plant.

Keywords: black start, PMSG based, wind turbine, voltage establishment, power balance, voltage reference

Edited by:
Liansong Xiong,
Nanjing Institute of Technology (NJIT), China

Reviewed by:
Pengda Wang,
Technical University of Denmark, Denmark
Weiyu Bao,
Shandong University, China

****Correspondence:***
Guohang Huang
mrhung33@outlook.com

Specialty section:
This article was submitted to Process and Energy Systems Engineering, a section of the journal Frontiers in Energy Research

Received: *22 March 2022*
Accepted: *12 April 2022*
Published: *11 May 2022*

Citation:
Ji X, Liu D, Hu P, Cao K, Jiang K, Huang G and Huang S (2022) Black Start and Voltage Establishment Strategy for PMSG-Based Wind Turbine. Front. Energy Res. 10:901708. doi: 10.3389/fenrg.2022.901708

1 INTRODUCTION

Black start is an inevitable starting procedure during the progress of grid restoration after a blackout happens (Chou et al., 2013; Erdiwansyah et al., 2021). Power sources with high reliability, such as thermal generators and hydro generators (Benato et al., 2019; Lindstrom, 1990), are usually used as backup power sources during black start. With the huge progress in virtual inertial control of wind power systems, wind turbines now can work as black start power sources (Pape and Kazerani, 2020). However, a complete black start scheme for wind turbines still requires reliable power supplies and stable voltage references, which are normally offered by backup diesel generators (Tang et al., 2017).

Generally, the first step of the black start procedure in a wind turbine is the startup of electrical subsystems. In order to boot up the electrical subsystems such as secondary circuits, pitch and yaw actuators, and cooling systems, the deployment of batteries or energy storage systems (Liu et al., 2021) is one of the best and most necessary solutions (Satpathy et al., 2014). After the startup of subsystems, the dc-link voltage must be established to make sure the power can be transferred from the generator to the line-side. The establishment of dc-link voltage is usually accomplished by a line-side converter or dc-link energy storage system. In the former case, the line-side voltage must be built by a backup motor before the grid line-converter can operate as expected, and a DFIG grid-forming technique using torque synchronization and voltage droop in the generator-side converter to form transient ac voltage has been proposed (Rodriguez-Amenedo et al., 2021), in which the dc-link

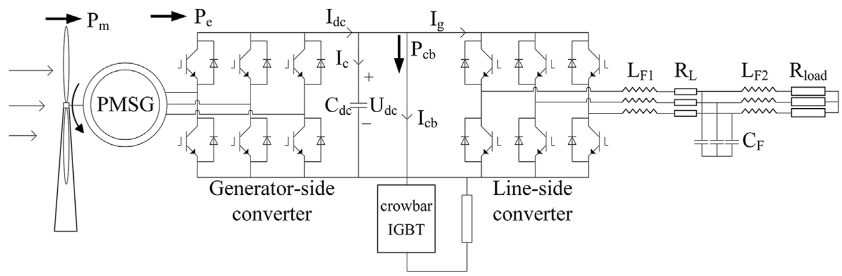

FIGURE 1 | Topology of the wind turbine during a black start.

voltage is maintained by the line-side converter; in the latter case, the capacity of energy storage system needs to be much larger since it will not only provide power to the subsystem but also help build the dc-link voltage (Xu et al., 2012; Deng et al., 2017; Sun et al., 2018).

When it comes to the circumstances with no extra back generators, a unique black start strategy for wind power plants using a centralized high-voltage dc-link converter has been proposed (Sakamuri et al., 2019; Saborío-Romano et al., 2019). By transmitting power from wind turbines to centralized high-voltage dc-link, the high centralized dc-link voltage can be established by the onshore high-voltage dc converter. However, the dc-link voltage of each single wind turbine which is supposed to be controlled by the generator-side converter in this study is considered constant. An active power-sharing method of wind turbine using the generator-side converter to control dc-link voltage and the grid-side converter to control active power is proposed (Fathabadi, 2017). The power balance is achieved between two wind turbines with the power-sharing strategy and one common local load, but the power flow between the grid and generator of one single turbine needs to be balanced during the effect of the power-sharing strategy with two turbines. A novel centralized control strategy based on the look-up table to ensure optimal power sharing is proposed (Alavi and Ghazi, 2022), using the optimal results from the centralized controller and data in the look-up table to achieve the optimal active power-sharing between multiple turbines. Though the optimal control command is obtained from the available wind power, it can still be a good reference when it comes to power balance with loads. In order to deal with the challenge caused by irregular, nonlinear, and nonstationary characteristics of wind power, an uncertainty modeling method based on the prediction of wind power is proposed (Yan et al., 2021), which, on the other hand, provides the possibility of grid-forming by wind power under variable wind speed and multiple loads.

From the recent research, two main challenges of black start control of wind turbines can be summarized: one is the establishment of dc and ac link voltage, and the other is the balance of power between generator and load. When a blackout happens with no backup generator, there is no grid line voltage, and dc-link voltage cannot be built by the line-side converter at the beginning. So, using the generator-side converter to build dc-link voltage is a better option. After the dc-link voltage rises and stays at a certain value, power begins to flow into the line-side converter, and

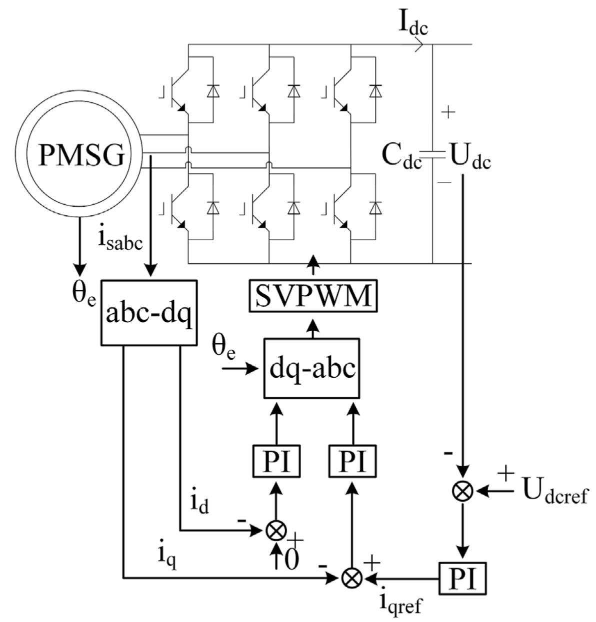

FIGURE 2 | Control strategy of the generator-side converter.

the line-side voltage starts to rise on local load, which leads to the problem of grid voltage control. Since the volt-ampere characteristic on fixed load under certain power input is also fixed, the line-side voltage forming problem can be turned into a power control problem for wind turbines, which is the main idea of this study.

The main contribution of this study is as follows: instead of backup diesel generators, fixed three-phase local loads are used to establish line-side voltage, which is much better for costs; the proposed power balance method is proposed to maintain the power balance between mechanical power input and electrical power consumption; the first wind turbine using the proposed black start control strategy in this study can be used as line-side voltage reference during the black start of a wind power plant, and the black start of the whole wind power plant can be completed with no extra backup generator. However, the power supply of subsystems in the first turbine still needs to be satisfied by power storage or battery.

In the proposed black start method for wind turbines, the dc-link voltage is established by the generator-side converter, and the line-side voltage is built by the line-side converter with power

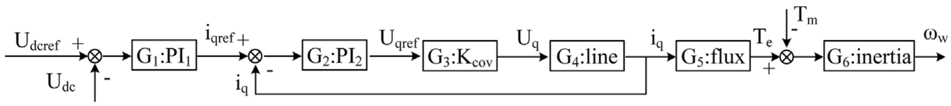

FIGURE 3 | Transfer diagram of the generator-side converter.

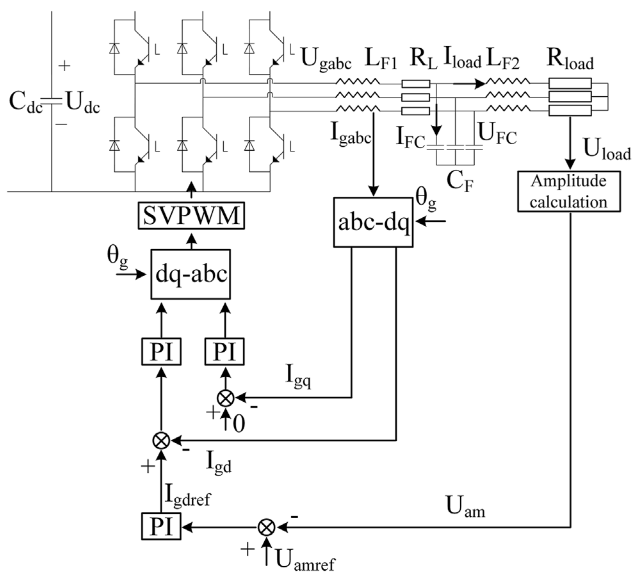

FIGURE 4 | Control strategy of the line-side converter.

balancing control of wind turbine and fixed load in ac line. The crowbar circuit is used to maintain the stability of rotor speed and dc-link voltage. By this method, the black start of a single wind turbine can be accomplished, and the line-side voltage can be established, offering voltage reference for the other wind turbines during the black start period of a wind power plant. The main content of this study is organized as follows. In **Section 2**, the main idea of this study and the topology of a wind turbine system during black start are briefly introduced. In **Section 3**, the black start control strategies of power converters and the power balance method in a wind turbine are detailed. In **Section 4**, 3 sets of simulations are carried out to testify to the validity of the proposed control strategy. In **Section 5**, the conclusion of the proposed method in this study is given and discussed.

2 SYSTEM DESCRIPTION

When a blackout happens, the line-side voltage falls to zero. The wind turbine needs to restart with no grid voltage reference, and the power from the generator needs to be consumed with the local load. The main topology of the wind turbine based on PMSG during the black start procedure is shown in **Figure 1**, the line-side converter is connected to the fixed load, and there is also an extra crowbar circuit within the dc-link.

Since there is no grid voltage during the whole black start procedure, the traditional MPPT control strategy of the full power converter is no longer suitable, the dc-link voltage can be controlled by the generator-side converter, and the line-side converter can be used to control the frequency, phase, and amplitude of the line-side voltage.

The local three-phase fixed load is designed for both power consumption and voltage establishment. With the exact information about the impedance characteristic of load and target amplitude and frequency of line-side voltage, the power demand of line-side voltage establishment can be calculated, which can be used to control the mechanical power capture of the wind turbine. During the black start, the wind turbine cannot operate at full power because the extra power cannot be absorbed by the grid. The power balance between the generator and load must be achieved by pitch angle control, as the pitch angle is the only controllable variable left to adjust mechanical power during black start. When the power balance is achieved steadily, the voltage of the line-side will be established and maintained at the designed value.

However, considering the power loss within the system, the power command calculated based on load and target line-side voltage cannot match the actual power need, which will cause the fluctuation in the rotor speed. In this study, the power command is designed higher than the calculated power, and the extra power is absorbed using the designed crowbar circuit to maintain the stability of rotor speed in a certain range.

3 MODELING AND CONTROL

In this section, the detailed model and control strategy of both the generator-side converter, the line-side converter, the wind turbine power capture method, and the crowbar circuit for a black start is presented.

3.1 System Modeling

As in **Figure 1**, the whole system contains a PMSG, a back-to-back full power converter, a crowbar circuit, an LCL filter, and a fixed load. The mathematical model of the system can be described based on **Figure 1**. The mechanical model of a PMSG-based wind turbine can be described as follows:

$$P_m = \frac{1}{2}\rho A V_w^3 C_P(\lambda,\beta), \tag{1}$$

$$C_P(\lambda,\beta) = C_1\left(\frac{C2}{\lambda} - C_3\beta - C_4\right)e^{-\frac{C_5}{\lambda_i}} + 0.0068\lambda, \tag{2}$$

$$\frac{1}{\lambda_i} = \frac{1}{\lambda + 0.008\beta} - \frac{0.035}{\beta^3 + 1}, \tag{3}$$

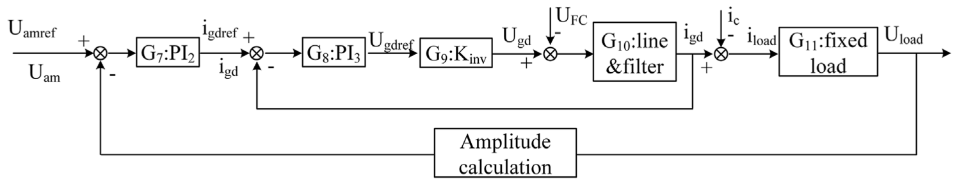

FIGURE 5 | Transfer diagram of the line-side converter.

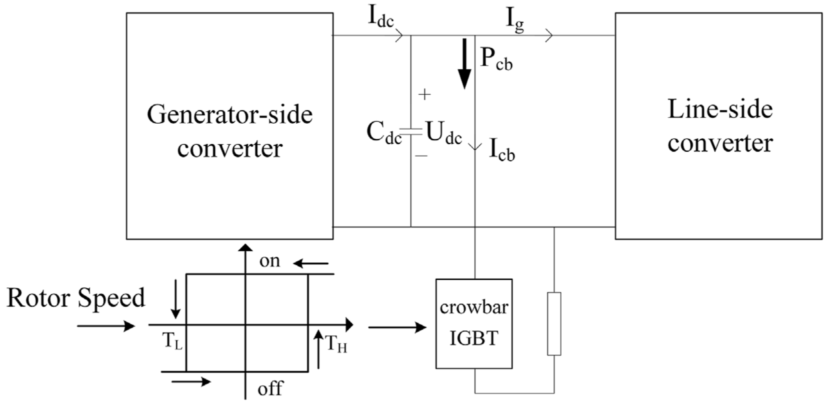

FIGURE 6 | Control strategy of the crowbar circuit.

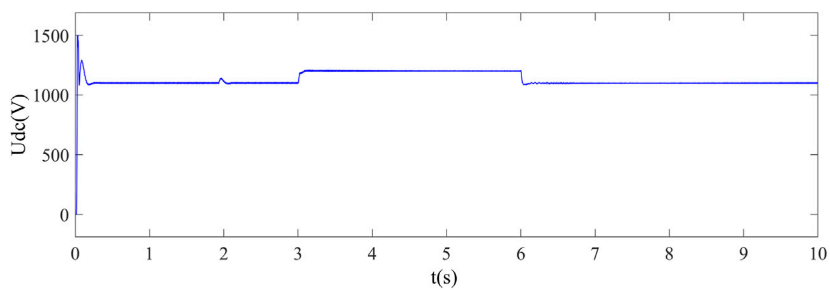

FIGURE 7 | Change of the dc-link voltage.

$$\lambda = \frac{R\omega_w}{V_w}. \tag{4}$$

In **Eqs 1–4** (Li et al., 2012; Fathabadi, 2017), the variable P_m is the mechanical power input, ρ is the air density, $A$is the rotation area of a wind turbine, V_w is the wind speed, C_p is the wind power coefficient, ω_w is the rotating speed of wind turbine and also can represent the rotor speed of PMSG, and λ is the tip speed ratio and β is the pitch angle. The constant values from C_1 to C_5 are 0.5173, 116, 0.4, 5, and 21.

As described in **equations (1)**-**(4)**, it is clear that wind power capture is related to the pitch angle and rotor speed.

The power flow within the wind power system can be written as

$$P_m - P_e = J\omega_w \frac{d\omega_w}{dt}, \tag{5}$$

$$P_e = i_{dc} U_{dc}, \tag{6}$$

$$P_e = P_{loss} + P_{load}. \tag{7}$$

In **Equation 5**, J is the inertial coefficient of PMSG.

During the black start, when dc-link voltage is stable, the electrical power P_e consists of load power P_{load} and power loss P_{loss}. The power unbalance between P_m and P_e can be reflected on ω_w.

3.2 Control of Back-To-Back Converter

The stability of dc-link voltage is quite important during the operation of the wind turbine. As is mentioned above, the line-side converter is not capable of maintaining the dc-link voltage

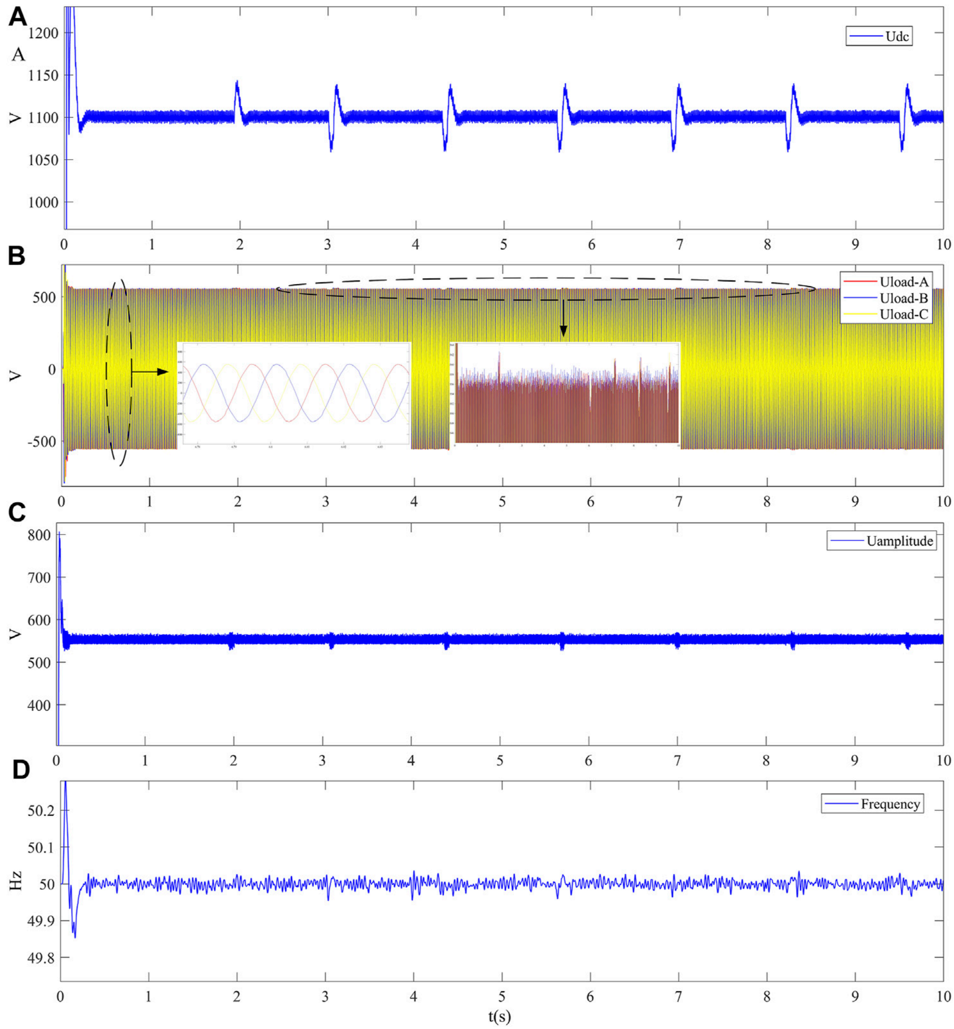

FIGURE 8 | The dc-link voltage, line-side voltage, and frequency in case 1. **(A)** The dc-link voltage **(B)** Detailed three-phase line-side voltage **(C)** Line-side voltage amplitude **(D)** line-side frequency.

during the initial transient non-voltage state. Instead, the generator-side converter can be used to control the dc-link voltage, the current equation of PMSG is represented as follows (Li et al., 2012):

$$\begin{cases} L_d \dfrac{di_d}{dt} = -Ri_d + \omega_e L_q i_q + u_d, \\ L_q \dfrac{di_q}{dt} = -Ri_q - \omega_e L_d i_d - \omega_e \varphi_f + u_q. \end{cases} \tag{8}$$

In **Equation 8**, L_d and L_q are the d-q axis inductance of PMSG, i_d and i_q are the d-q axis current component of PMSG, ω_e is the electrical angle frequency, u_d and u_q are the d-q axis terminal voltage component , and φ_f is the permanent magnet flux linkage of PMSG. Based on **Equation 8**, the control scheme of the generator-side converter is given in **Figure 2**.

As shown in **Figure 2**, the generator-side converter uses a dc-link voltage outer loop and current inner loop to achieve the stability of dc-link voltage, the d-axis current component is controlled to 0 to achieve the maximum torque. The transfer diagram of the generator-side converter is shown in **Figure 3**. In **Figure 3**, G_1 and G_2 represent the gain of the PI controller, G_3 is the gain of the generator-side converter which is normally regarded as an inertial link. G_4 represents the stator winding, G_5 represents the effect of permanent magnet flux linkage, and G_6 represents the inertia coefficient of PMSG and wind turbine.

The dc-link voltage in **Figure 1** can be described as

$$\begin{cases} C \dfrac{dU_{dc}}{dt} = i_c, \\ i_c = i_{dc} - i_{cb} - i_g. \end{cases} \tag{9}$$

From **Equation 9** it is clear that the changes in dc-link voltage are related to the control of line-side and crowbar control. When the dc-link voltage is relatively stable, the power generated can

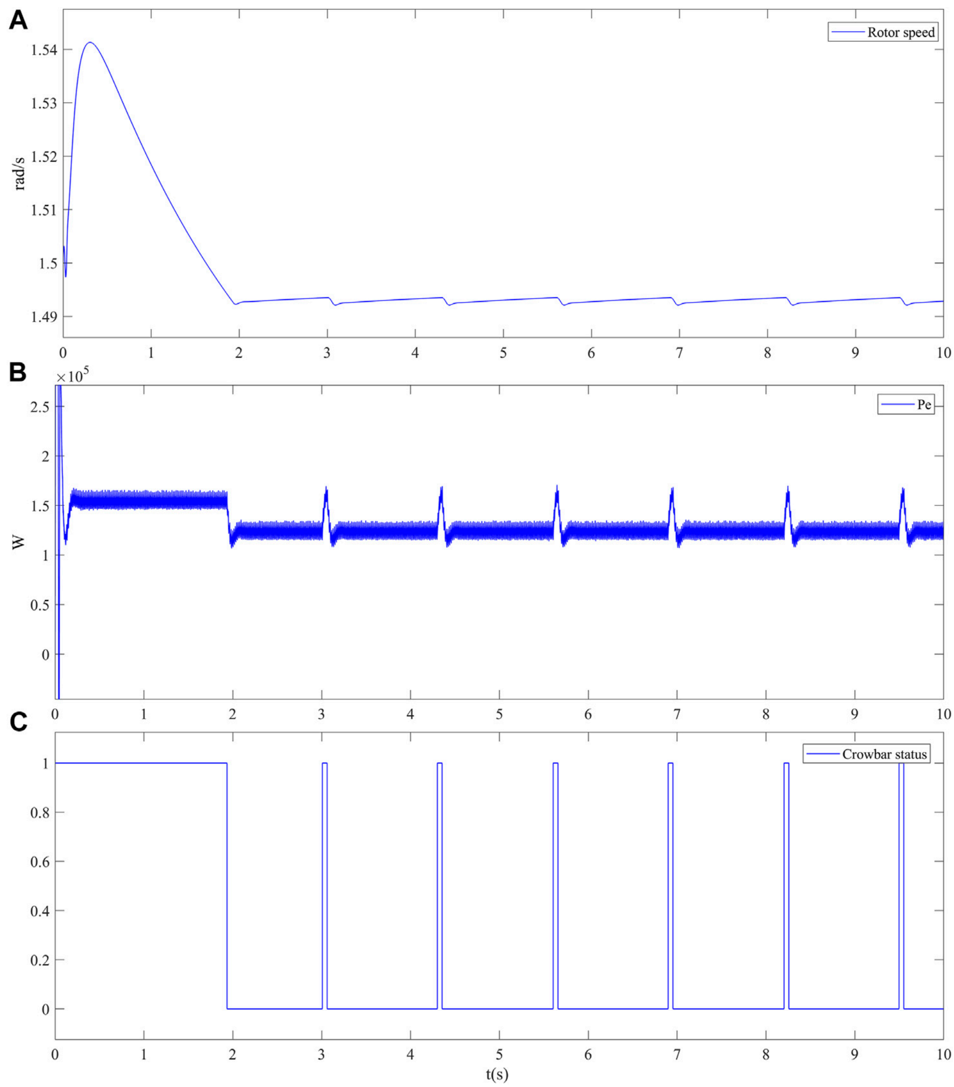

FIGURE 9 | The rotor speed, electrical power, and crowbar status in case 1. **(A)** The rotor speed **(B)** Electrical power Pe **(C)** Crowbar status.

flow into the line-side, and the power flow can be described using **Eqs (5)** and **(6)**.

The line-side converter is used to control the frequency and amplitude of output voltage, offering voltage reference for the other turbines. The current equation is given as follows (Ashourianjozdani et al., 2018):

$$\begin{cases} L_{gd}\dfrac{di_{gd}}{dt} = -Ri_{gd} + \omega_g L_{gq} i_{gq} + u_{gd} - e_d, \\ L_{gq}\dfrac{di_{gq}}{dt} = -Ri_{gq} - \omega_g L_{gd} i_{gd} + u_{gq} - e_q. \end{cases} \quad (10)$$

In **Equation 10**, L_{gd} and L_{gq} are the d-q axis line-side inductance, i_{gd} and i_{gq} are the d-q axis component of line-side output current, ω_g is the line-side frequency which is controlled to 50Hz, u_{gd} and u_{gd} are the d-q axis component of the line-side terminal voltage, and the line-side voltage source e_d and e_q are set to 0 because there is no grid voltage during the whole black start procedure.

Based on **Equation 10**, the control diagram can be obtained in **Figure 4**. As in **Figure 4**, the line-side converter uses phase-to-ground voltage amplitude outer loop and current inner loop, the q-axis component is set to zero to improve the power factor. The transfer diagram of the line-side converter is shown in **Figure 5**.

In **Figure 5**, G_7 and G_8 represent the gain of PI controller, G_9 is the transfer function of the grid-side converter which is also treated as an inertia link, G_{10} represents the power loss in line before the capacitor branch of LCL filter, and G_{11} is the fixed load designed for voltage establishment.

Ignoring the voltage of the filter capacitor, the transfer function of **Figure 5** can be obtained as follows:

$$\frac{U_{amref}(s)}{U_{am}(s)} = \frac{G_8(s)G_9(s)G_{10}(s)G_{11}(s)}{1 + G_8(s)G_9(s)G_{10}(s) + G_8(s)G_9(s)G_{10}(s)G_{11}(s)}. \quad (11)$$

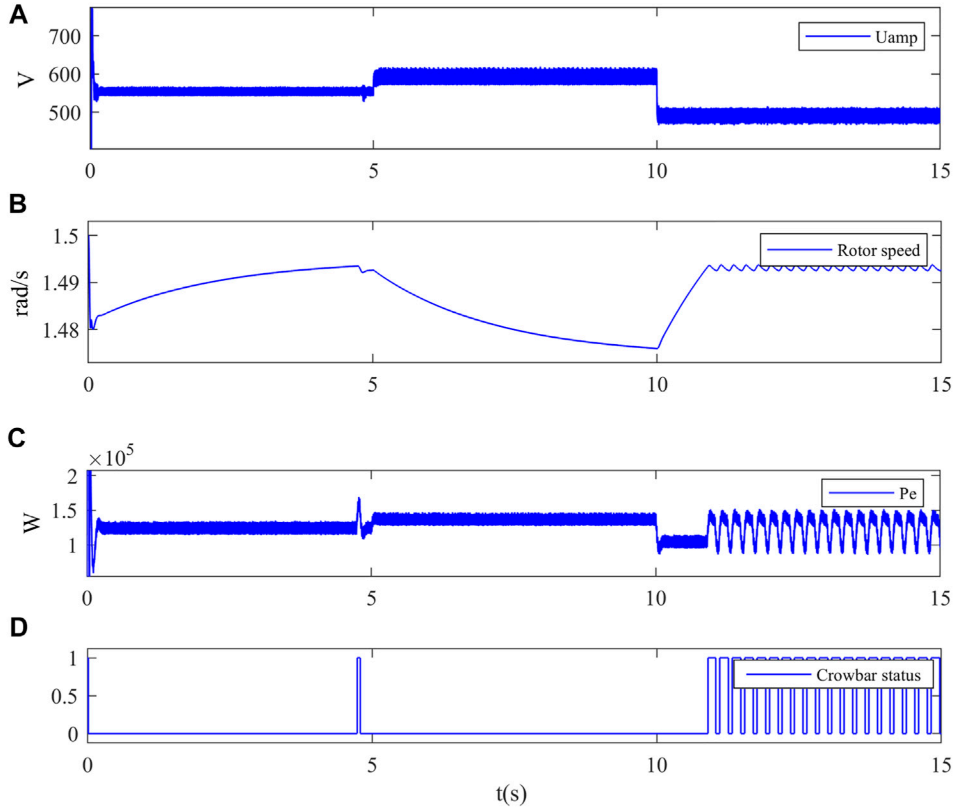

FIGURE 10 | The line-side voltage amplitude, rotor speed, electrical power, and crowbar status in case 2. **(A)** Line-side voltage amplitude **(B)** Rotor speed **(C)** Electrical power Pe **(D)** Crowbar status.

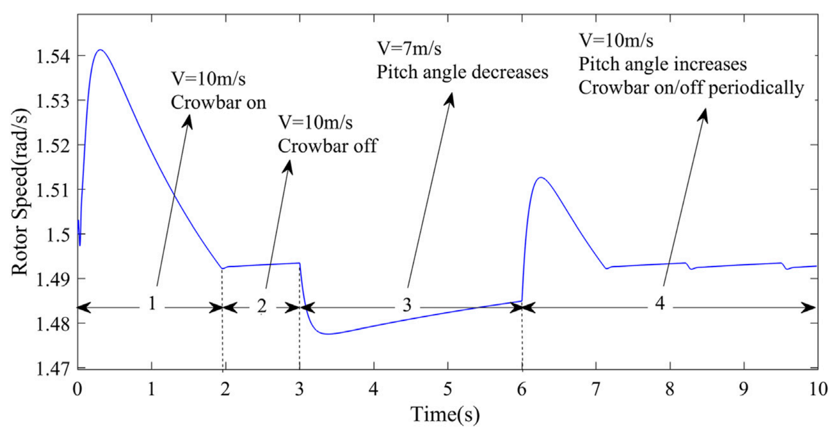

FIGURE 11 | Change of the rotor speed in case 3.

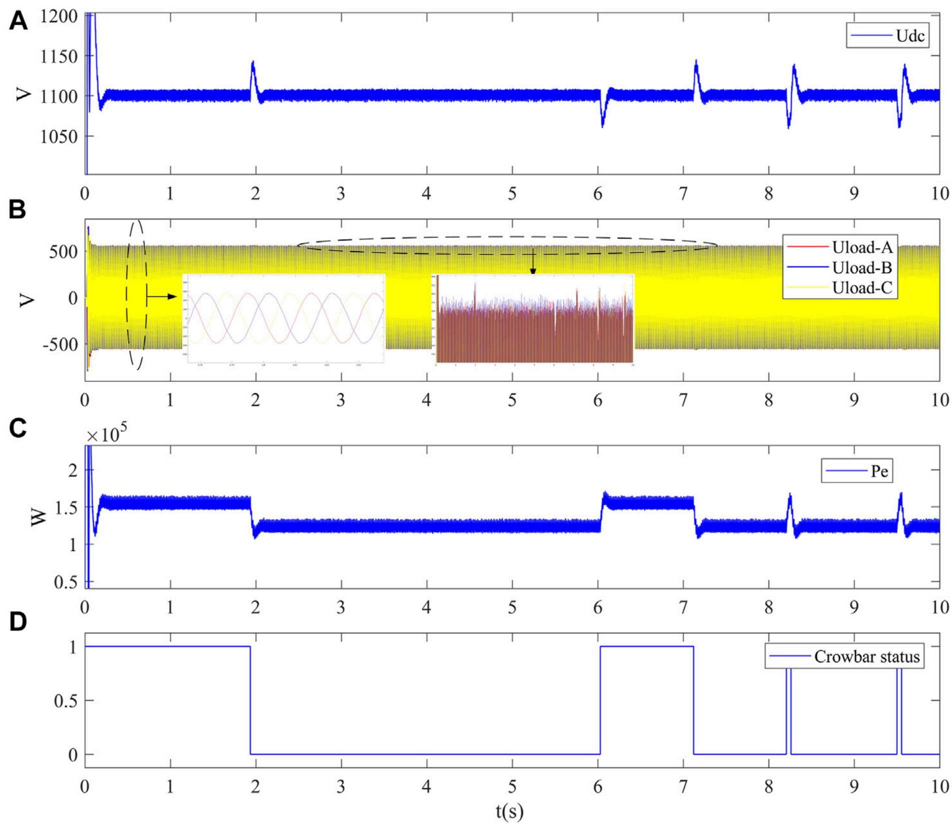

FIGURE 12 | The DC-link voltage, line-side voltage, power, and crowbar status in case 3. **(A)** The dc-link voltage **(B)** Detailed three-phase line-side voltage **(C)** Electrical power Pe **(D)** Crowbar status.

Eq. 11 can be regarded as a phase shift, and the amplitude of load voltage will be controlled as the command value. Because there is no line voltage reference, the PLL is no longer needed, and the phase signal θ_g which is used to convert the coordinate is calculated based on the target frequency.

3.3 Voltage Establishment and Power Balance Control

With the control structure built by the back-to-back converter, the amplitude and frequency of voltage on load can be controlled to a certain designed value, which can offer voltage reference during the black start to multiple wind turbines. In order to maintain the voltage level on load, the mechanical power input must be high enough to make sure the power flow within the converter can satisfy the power demand on load. When the amplitude and frequency of load voltage are determined, the mathematical relationship between voltage, load, and three-phase power on load can be represented as

$$S_{load} = 3U_{amp}^2 \big/ Z_{load}. \tag{12}$$

In **Equation 12**, S_{load} is the apparent power on load, U_{amp} is the phase-to-ground voltage amplitude on load, and Z_{load} is the impedance of the load. With a fixed resistive load, the power under a certain voltage level can be calculated as

$$P_{load} = 3U_{amp}^2 \big/ R_{load}. \tag{13}$$

Also, the space state equation of the line-side in **Figure 4** can be obtained as

$$\begin{cases} U_g = L_{F1}\dfrac{dI_g}{dt} + I_g R_L + U_{FC}, \\ U_{FC} = L_{F2}\dfrac{dI_{load}}{dt} + U_{load}, \\ U_{load} = I_{load}R_{load}, \\ I_{FC} = C_F\dfrac{dU_{FC}}{dt}. \end{cases} \tag{14}$$

In **Equation 14**, U_g and I_g represent the U_{gabc} and I_{gabc} in **Figure 4**, the power loss of the line-side can be obtained from **Equation 14** as

$$P_{lossL} = I_g L_{F1}\frac{dI_g}{dt} + I_g^2 R_L + I_{load}L_{F2}\frac{dI_{load}}{dt} + U_{FC}C_F\frac{dU_{FC}}{dt}. \tag{15}$$

Unlike power loss of line-side, power loss that exists in the winding of PMSG is hard to quantify. In order to simplify the analysis in this study, the power loss in PMSG is symbolized by P_{lossg}, therefore the power loss and electrical power can be described using **the** following equation:

$$\begin{cases} P_{loss} = P_{lossL} + P_{lossG}, \\ P_e = P_{loss} + P_{load}. \end{cases} \tag{16}$$

The constant voltage on load means stable power consumption on the line-side. The load voltage can maintain stability as long as P_e can be supplied by the generator. The line-side voltage can be supported when P_m meets the need of P_e in **Equation 16**; otherwise, the rotor speed of PMSG will change because of the power unbalance until the system loses its control stability.

In order to make sure that P_m meets P_e, the power capture of a wind turbine is the only controllable link left if there is no power storage. As in **Eqs 1**, **2**, P_m can be controlled by pitch angle control and rotor speed control. If the power loss in PMSG can be ignored, the ideal power balance can be described with the following:

$$\begin{cases} P_{mi} = \frac{1}{2}\rho A V_{wi}^3 C_{pi}(\lambda_i, \beta_i), \\ P_{ei} = P_{lossi} + P_{loadi}, \\ P_{mi} = P_{ei}. \end{cases} \tag{17}$$

In **Equation 17**, the letter subscript i means the ideal situation. Under the ideal situation, the balance between P_m and P_e is achieved by pitch control of the wind turbine, the wind power coefficient C_p is used to describe P_m based on the wind speed V_{wi}, initial rotor speed ω_{wi}, and the data in the look-up table in the theoretical analysis. The rotor speed ω_{wi} will maintain steady because there is no delay in pitch control under an ideal situation, and the power balance can be achieved as long as the system operates.

However, considering the power loss in PMSG and the delay in pitch control, it is difficult to maintain the power balance as the ideal situation, as a result ω_w will fluctuate with power unbalance, damaging the stability of the system. In case of that, a power balance control strategy using pitch control and crowbar circuit to maintain the relative stability of rotor speed is proposed.

When wind speed reaches the cut-in speed, the brake of the wind turbine should be released to make sure there is enough rotational kinetic energy saved in the rotor, otherwise, the mechanical power will be smaller than electrical power, and the capacitor charging and load voltage establishment will not be completed. After the initial rotor kinetic energy satisfies the electrical power need, pitch angle control starts to react to the power command to make sure wind power captured in **Equation 1** is higher than P_{ei} in **Equation 17**. The updated C_p value is obtained based on the transient real-time rotor speed, tip speed ratio, and look-up table.

Based on **Equation 5**, the rotor speed will increase because of the power unbalance. A designed crowbar circuit is used to consume the extra power, the power consumed in the crowbar circuit can be described using **the** following equation:

$$\begin{cases} P_{cb} = U_{dc}^2 / Z_{cb} & (crowbar\ on), \\ P_{cb} = 0 & (crowbar\ off). \end{cases} \tag{18}$$

the power of the crowbar circuit must satisfy the following constraint:

$$\begin{cases} P_m > P_{lossi} + P_{loadi} \\ P_m < P_{cb} + P_{lossi} + P_{loadi} \end{cases}. \tag{19}$$

When the power flow satisfies **Equation 19**, the rotor speed can be stabled within a certain range. The control of the crowbar circuit based on the detected rotor speed is shown in **Figure 6**. In **Figure 6**, T_L and T_H are the threshold values.

When there is a sudden disturbance in the system, the pitch angle control reacts to the power disturbance at first. When the mechanical power input is adjusted by pitch control to balance with the electrical power, the crowbar circuit is then activated to adjust the rotor speed after the power balance is relatively accomplished. The change in rotor speed caused by power imbalance during power regulation by pitch control can be compensated by a crowbar. In other words, the crowbar circuit works as a secondary regulator. However, the crowbar circuit in this work is necessary because the change in rotor speed during the power regulation by pitch control must be regulated so that the control stability issues can be avoided.

4 RESULTS

4.1 Case 1: Wind Speed Fixed Situation

In this section, the simulation results in the wind turbine system shown in **Figure 1** are given. The designed phase-to-phase line-side voltage RMS is 690 V, and the load value is fixed so that the power on the load changes with the designed load voltage. The results are obtained using the MATLAB/Simulink.

First, the dc-link voltage is set to 1100 V at t = 0s, 1200 V at t = 3 s, then back to 1100 V at t = 6 s to verify the control of generator-side. The result is shown in **Figure 7**.

As in **Figure 7**, the dc-link voltage can follow the control reference as expected. The wind speed is set to 10 m/s, the initial rotor speed of the wind turbine is set to 1.5 rad/s because in reality the brake of the wind turbine should be released and the initial rotor kinetic energy should be high enough to make sure the PMSG will not stall against the electrical power and lose the operation stability during black start. The dc-link voltage, line-side voltage, line-side frequency, and power are shown in **Figure 8**.

As in **Figure 8A**, the dc-link voltage is controlled to 1100 V, and the specifics of the line-side voltage are presented in **Figure 8B–D**. As in **Figure 8C**, the phase-to-ground voltage amplitude of load voltage is controlled to 563 V, and the frequency in **Figure 8D** is maintained as 50 Hz. When the crowbar circuit is activated, the power flow satisfies **Equation 11** which causes the periodic fluctuation in electrical power.

The changes in the rotor speed and power are given in **Figures 9A,B**. During t = 0–0.3 s, P_e rises to a transient peak level and returns to stability very quickly because the line-side voltage and dc-link voltage are under control in a short time. The rotor speed increases at first and then decreases because the initial rotor speed of 1.5 rad/s is at the right side of the maximum power point so that P_m decreases when rotor speed increases. When P_m falls lower thanP_e, the rotor speed ω_w will decrease until it is lower than the threshold valuesT_L. Then the crowbar circuit will start to work periodically. The status of the crowbar circuit is presented in **Figure 9C**. Because the rotor speed is higher than the trigger threshold valueT_H, the crowbar IGBT is kept open at the beginning till the rotor speed decreases toT_L, which explains the reduction in P_e at about 1.9 s.

4.2 Case 2: Variable Line-Side Voltage

In this case, the reference value of phase-to-ground voltage amplitude of load is set to 563 V at t = 0 s, 600V at t = 5 s, and 500 V at t = 10 s. However, the mechanical power command is not adjusted with the change of line-side voltage so that the system dynamics can be shown more independently. The status of load phase-to-ground voltage is shown in **Figure 10A**, the changes in rotor speed and power are shown in **Figures 10B,C**, and the status of the crowbar circuit is given in **Figure 10D**. The crowbar circuit is not activated until about t = 5 s when the rotor speed is higher than the threshold. Then, P_e is higher than P_m after t = 5 s because the line-side voltage rises, which makes the rotor speed continue to drop and the crowbar circuit, therefore, is deactivated. At t = 10 s, the line-side voltage drops and P_e decreases, which makes the rotor speed rises till the crowbar circuit is activated periodically.

4.3 Case 3: Change of Wind Speed

In this case, the wind speed changes from 10 m/s to 7 m/s at t = 3 s, and then changes back to 10 m/s at t = 6 s, the change of rotor speed is shown in **Figure 11**. As in **Figure 11**, when wind speed changes at t = 3 s and t = 6 s, the delay of pitch action causes a transient power gap between P_e andP_m, thus rotor speed changes with power. After wind speed returns to 10 m/s, the crowbar circuit can still work as a rotor speed stabilizer.

The dc-link voltage, line-side voltage, and power are presented in **Figure 12**. In **Figure 12**, it is clear that instead of changes in wind speed, the changes in P_e are directly related to the changes in U_{dc} and U_{load}, which improves that as long as the electrical power can be offered by the wind power input and rotor kinetic energy storage, the voltage of dc-link and line-side can be maintained by converter without being affected by change of rotor speed. Instead, the rotor speed can be treated as a variable of the state which reflects the power unbalance between P_e and P_m.

5 CONCLUSION

In this study, a control strategy of the black start and line-side voltage establishment for PMSG-based wind power system is proposed. The dc-link voltage is stabled using the generator-side converter, and the line-side voltage is controlled by the line-side converter. The pitch angle is used to balance mechanical power and electrical power, and an extra crowbar circuit is applied to maintain the rotor speed. The proposed black start control strategy and the line-side voltage establishment method should be carried out in the following order:

Step 1. Calculating the load power based on the desired line-side voltage level and local load configuration.

Step 2. Releasing the brake device of the wind turbine when wind speed reaches the cut-in speed, initiating the controller of the generator-side converter, the line-side converter, and the crowbar circuit after the rotor speed reaches a point under which the initial rotor kinetic energy can match the load power need in step 1.

Step 3. : Adjusting the pitch angle using a power closed loop to make sure the mechanical power input and the electrical power demand match the description in **Eq. 19**. At this point, the rotor speed will rise and then be controlled periodically by the crowbar circuit.

Step 4. When the line-side voltage reaches the designed value, the other wind turbines can follow up their procedures using the line-side voltage of the first wind turbine as a reference, which will be testified in our next work.

By the proposed control strategy, the problems about the stability of the dc-link voltage and the establishment of line-side voltage can be solved. The simulation results show the validity of the proposed method, and rotor speed can be used to check the unbalance between the electrical power and mechanical power. Once the line-side voltage is established, more wind turbines can start up using the voltage reference built by the one using the proposed method in this study.

DATA AVAILABILITY STATEMENT

The raw data supporting the conclusions of this article will be made available by the authors, without undue reservation.

AUTHOR CONTRIBUTIONS

XJ: designing of the main control strategy. DL: modifying of the topology. PH: construction of simulation. KC: designing of the simulation control group. KJ: writing of the original manuscript. GH: revision of the manuscript. SH: optimization of the control strategy.

REFERENCES

Alavi, S. M., and Ghazi, R. (2022). A Novel Control Strategy Based on a Look-Up Table for Optimal Operation of MTDC Systems in Post-contingency Conditions. *Prot. Control Mod. Power Syst.* 7, 4. doi:10.1186/s41601-022-00224-3

Ashourianjozdani, M., Lopes, L. A. C., and Pillay, P. (2018). Power Electronic Converter Based PMSG Emulator: A Testbed for Renewable Energy Experiments. *IEEE Trans. Ind. Appl.* 54, 3626–3636. doi:10.1109/TIA.2018.2819618

Benato, R., Bruno, G., Sessa, S. D., Giannuzzi, G. M., Ortolano, L., Pedrazzoli, G., et al. (2019). A Novel Modeling for Assessing Frequency Behavior during a Hydro-To-Thermal Plant Black Start Restoration Test. *IEEE Access* 7, 47317–47328. doi:10.1109/ACCESS.2019.2909321

Chou, Y.-T., Liu, C.-W., Wang, Y.-J., Wu, C.-C., and Lin, C.-C. (2013). Development of a Black Start Decision Supporting System for Isolated

Power Systems. *IEEE Trans. Power Syst.* 28, 2202. doi:10.1109/TPWRS.2013.2237792

Deng, F., Dong, L., Chen, Z., and Su, P. (2017). Control Strategy of Wind Turbine Based on Permanent Magnet Synchronous Generator and Energy Storage for Stand-Alone Systems. *Chin. J. Electr. Eng.* 3, 51–62. doi:10.23919/CJEE.2017.7961322

Erdiwansyah, M., Mahidin, H., Husin, H., Nasaruddin, fnm., Zaki, M., and Muhibbuddin, fnm. (2021). A Critical Review of the Integration of Renewable Energy Sources with Various Technologies. *Prot. Control Mod. Power Syst.* 6, 3. doi:10.1186/s41601-021-00181-3

Fathabadi, H. (2017). Novel Maximum Electrical and Mechanical Power Tracking Controllers for Wind Energy Conversion Systems. *IEEE J. Emerg. Sel. Top. Power Electron.* 5, 1739–1745. doi:10.1109/JESTPE.2017.2727978

Li, S., Haskew, T. A., Swatloski, R. P., and Gathings, W. (2012). Optimal and Direct-Current Vector Control of Direct-Driven PMSG Wind Turbines. *IEEE Trans. Power Electron.* 27, 2325–2337. doi:10.1109/TPEL.2011.2174254

Lindstrom, R. R. (1990). Simulation and Field Tests of the Black Start of A Large Coal-Fired Generating Station Utilizing Small Remote Hydro Generation. *IEEE Trans. Power Syst.* 5, 162–168. doi:10.1109/59.49101

Liu, S., Zhou, C., Guo, H., Shi, Q., Song, T. E., Schomer, I., et al. (2021). Operational Optimization of a Building-Level Integrated Energy System Considering Additional Potential Benefits of Energy Storage. *Prot. Control Mod. Power Syst.* 6, 4. doi:10.1186/s41601-021-00184-0

Pape, M., and Kazerani, M. (2020). Turbine Startup and Shutdown in Wind Farms Featuring Partial Power Processing Converters. *IEEE Open J. Power Energy* 7, 254–264. doi:10.1109/OAJPE.2020.3006352

Rodriguez-Amenedo, J. L., Gomez, S. A., Martinez, J. C., and Alonso-Martinez, J. (2021). Black-Start Capability of DFIG Wind Turbines through a Grid-Forming Control Based on the Rotor Flux Orientation. *IEEE Access* 9, 142910–142924. doi:10.1109/ACCESS.2021.3120478

Saborio-Romano, O., Bidadfar, A., Sakamuri, J. N., Goksu, O., and Cutululis, N. A. (2019). "Primary Frequency Response from Offshore Wind Farms Connected to HVdc via Diode Rectifiers," in Proceeding of the 2019 IEEE Milan PowerTech, Milan, Italy, June 2019 (IEEE). doi:10.1109/PTC.2019.8810907

Sakamuri, J. N., Bidadfar, A., Saborio-Romano, O., Jain, A., and Cutululis, N. A. (2019). Black Start by HVdc-Connected Offshore Wind Power Plants. Proceeding of the 45th Annual Conference of the IEEE Industrial Electronics Society, Lisbon, Portugal, Oct. 2019 (IEEE). doi:10.1109/IECON.2019.8927615

Satpathy, A. S., Kishore, N. K., Kastha, D., and Sahoo, N. C. (2014). Control Scheme for a Stand-Alone Wind Energy Conversion System. *IEEE Trans. Energy Convers.* 29, 418–425. doi:10.1109/TEC.2014.2303203

Sun, L., Peng, C., Hu, J., and Hou, Y. (2018). Application of Type 3 Wind Turbines for System Restoration. *IEEE Trans. Power Syst.* 33, 3040–3051. doi:10.1109/TPWRS.2017.2762009

Tang, Y., Dai, J., Wang, Q., and Feng, Y. (2017). Frequency Control Strategy for Black Starts via PMSG-Based Wind Power Generation. *Energies* 10, 358. doi:10.3390/en10030358

Xu, G., Xu, L., Morrow, D. J., and Chen, D. (2012). Coordinated DC Voltage Control of Wind Turbine with Embedded Energy Storage System. *IEEE Trans. Energy Convers.* 27, 1036–1045. doi:10.1109/TEC.2012.2220361

Yan, C., Tang, Y., Dai, J., Wang, C., and Wu, S. (2021). Uncertainty Modeling of Wind Power Frequency Regulation Potential Considering Distributed Characteristics of Forecast Errors. *Prot. Control Mod. Power Syst.* 6, 22. doi:10.1186/s41601-021-00200-3

Conflict of Interest: Author XJ is employed by State Grid Hubei Electric Power CO., LTD.; Authors DL, PH, KC, and KJ are employed by Electric Power Research Institute, Hubei Electric Power Company, State Grid; authors GH and SH are employed by the College of Electrical and Information Engineering, Hunan University. This study received funding from the science and technology project of the State Grid Corporation of China, project number 4000-202122070A-0-0-00. The funder had involvement in the study design, collection, and data analysis. All authors declare no other competing interests.